of related delocalized clusters but with higher Fe:Mo ratios. Lastly, the set of electronic features now determined for $MoFe_3S_4$ clusters provides a meaningful test of any theoretical electronic structural model. One such model, based on the Xα approach, has been developed.[51]

Acknowledgment. This research was supported at Harvard University (Grant CHE 81-06017) and the Francis Bitter National Magnet Laboratory by the National Science Foundation. We thank Prof. D. Coucouvanis for a preprint of ref 31 and Dr. B. K. Burgess for a sample of FeMo-co.

Registry No. 1, 86645-74-1; 7, 86667-97-2; $[MoFe_3S_4(SEt)_3(Pr_2cat)(Me_2SO)]^{2-}$, 86645-75-2; $(Et_4N)_4[Mo_2Fe_6S_8(S\text{-}p\text{-}C_6H_4Cl)_6((al)_2cat)_2]$, 82247-34-5; $(Et_4N)_3[MoFe_3S_4(S\text{-}p\text{-}C_6H_4Cl)_4((al)_2cat)]$, 80789-40-8; $[MoFe_3S_4(S\text{-}p\text{-}C_6H_4Cl)_3((al)_2cat)CN]^{3-}$, 80702-97-2; $[WFe_3S_4(S\text{-}p\text{-}C_6H_4Cl)_3((al)_2cat)CN]^{3-}$, 84130-55-2; $[MoFe_3S_4(S\text{-}p\text{-}C_6H_4Cl)_3((al)_2cat)(MeCN)]^{2-}$, 80702-98-3; $[MoFe_3S_4(SPh)_3(Pr_2cat)(Me_2SO)]^{2-}$, 86645-76-3.

(51) Cook, M. D.; Karplus, M., manuscript in preparation.

Contribution from the Fachbereich Chemie der Phillips-Universität, D-3550 Marburg 1, West Germany

Cu^{2+} in Five-Coordination: A Case of a Second-Order Jahn-Teller Effect. 1. Structure and Spectroscopy of the Compounds $Cu(terpy)X_2 \cdot nH_2O$

W. HENKE, S. KREMER, and D. REINEN*

Received December 29, 1982

Five-coordinate Cu^{2+} complexes were studied by means of ligand field and EPR spectroscopy in the compounds $Cu(terpy)X_2 \cdot nH_2O$ ($X = Cl^-, Br^-, I^-, NO_2^-, NO_3^-, F^-$). In addition single-crystal structure analyses of $Cu(terpy)Cl_2 \cdot nH_2O$ ($n = 0$, $P2_1/a$; $n = 1$, $C2/c$) were performed. The CuN_3Cl_2 polyhedra are essentially tetragonal pyramids, though the influence of the rigid tridentate terpy ligand leads to deviations from this geometry. The pyramids are strongly elongated with apical Cu-Cl spacings of ≃2.50 Å and relatively short equatorial bonds. Similar geometries are derived from the spectroscopic data of most of the cited compounds. Apparently the elongated tetragonal bipyramid is the favored geometry for five-coordinate Cu^{2+} complexes of the considered constitution. In the EPR spectra of some compounds exchange coupling between Cu^{2+} polyhedra of different orientations in the unit cell is observed. From the cooperative **g** tensors the molecular *g* values could be derived, with use of the crystallographic data.

Introduction

During the preparation of the compounds $Cu(terpy)_2X_2 \cdot nH_2O$ with $Cu(terpy)_2^{2+}$ cations, in which Cu^{2+} is bonded to six N atoms in a strongly distorted octahedral coordination,[1,2] we observed the formation of the complexes $Cu(terpy)X_2 \cdot nH_2O$ also. In these compounds the Cu^{2+} ions are bonded to three N atoms and two additional ligands. While the symmetry of the $Cu(terpy)_2$ entities is determined by a strong first-order Jahn-teller effect, the stereochemistry of the five-coordinated complexes can be discussed on the basis of a second-order Jahn-Teller effect with respect to the alternative trigonal-bipyramidal (TBP) and square-pyramidal (SP) geometry.[3] Electrostatic calculations[4,5] show that the TBP geometry—with longer axial than equatorial bond lengths—is energetically slightly more stable than the SP geometry with a contracted apical bond distance, if electronic effects are absent. We are interested in the question of whether the presence of the d^9 cation Cu^{2+} will influence these relative stabilities and will consider this problem on a more general basis elsewhere.[3] In the following we will report about the crystal structures of $Cu(terpy)Cl_2 \cdot nH_2O$ with $n = 1$ and $n = 0$ and give the results of spectroscopic measurements on a series of mostly newly prepared complexes, $Cu(terpy)X_2 \cdot nH_2O$ ($X = Cl^-, Br^-, I^- NO_2^-, NO_3^-, F^-$). An interesting aspect in this connection is the correlation of the EPR spectra and the coordination geometries. This matter is rather complicated, however, because exchange interactions between Cu^{2+} polyhedra with different orientations in the unit cell may be present.

Experimental Section

Preparation of the Compounds $Cu(terpy)_mX_2 \cdot nH_2O$. X = Cl^-. Concentrated solutions of $CuCl_2 \cdot 2H_2O$ in water and terpyridine in ethanol are united in the molar ratio 1:2. The green precipitate corresponds to $m = 2$ with varying water content ($n \simeq 2$-4).[1,2] The solid compounds decompose to the complex with $m = 1$ and terpyridine, if they are sharply dried over P_2O_5 or cautiously heated. The process is reversible, as we have found by means of X-ray analysis and ligand field (Figure 1) and EPR spectroscopy. If one dissolves $CuCl_2 \cdot 2H_2O$ and terpyridine (molar ratio 1:1) in boiling water (concentrated solution), green crystals of $Cu(terpy)Cl_2$ with $n = 0$ and $n = 1$ form side by side on cooling. The dark green crystals, which precipitate from the mother liquor if it is slowly evaporated in air at room temperature, have exclusively $n = 1$, however. The compound with $n = 0$ is not hygroscopic but stable even in moist air. It had been prepared and characterized by X-ray powder diagrams earlier.[6] Anal. Calcd for $m = 2$, $n = 4$: C, 53.5; H, 4.5; N, 12.5. Found: C, 53.4; H, 4.0; N, 12.4. Calcd for $m = 1$, $n = 1$: C, 46.6; H, 3.3; N, 10.8. Found: C, 46.7; H, 3.4; N, 10.9. Calcd for $m = 1$, $n = 0$: C, 49.0; H, 3.0; N, 11.4. Found: C, 48.8; H, 3.1; N, 11.2.

X = Br^-, I^-. The light green compound $Cu(terpy)Br_2$ is accessible indirectly by careful heating of $Cu(terpy)_2Br_2 \cdot 3H_2O$ or directly from hot solutions of $Cu(NO_3)_2$ and terpyridine by precipitation with a slight excess of KBr, by a procedure analogous to that described above. Brown crystals of $Cu(terpy)I_2$ are obtained by precipitation with KI. Anal. Calcd for X = Br^-: C, 39.5; H, 2.4; N, 9.2. Found: C, 39.8;

(1) W. Henke and D. Reinen, *Z. Anorg. Allg. Chem.*, **436**, 198 (1977).
(2) R. Allmann, W. Henke, and D. Reinen, *Inorg. Chem.*, **17**, 378 (1978).
(3) D. Reinen and C. Friebel, *Inorg. Chem.*, in press.
(4) R. J. Gillespie and R. S. Nyholm, *Q. Rev., Chem. Soc.*, **11**, 339 (1957).
(5) D. L. Kepert in "Inorganic Chemistry Concepts", Vol. 6, Springer-Verlag, New York, 1982, p 36.
(6) C. M. Harris, N. N. Lockyer, and N. C. Stephenson, *Aust. J. Chem.* **19**, 1741 (1966).

0020-1669/83/1322-2858$01.50/0

Table I. Positional and Thermal Parameters for $Cu(terpy)Cl_2$

atom	x/a	y/b	z/c	B_{11}	B_{22}	B_{33}	B_{12}	B_{13}	B_{23}
Cu1	0.10969 (5)	0.0669 (1)	0.20687 (7)	1.50 (3)	2.04 (3)	2.29 (3)	−0.12 (3)	0.39 (2)	0.01 (3)
Cl1	0.2357 (1)	0.0227 (2)	0.1356 (2)	1.97 (7)	3.25 (9)	4.14 (9)	0.08 (6)	1.33 (6)	−0.13 (7)
Cl2	0.1286 (1)	0.3144 (2)	0.3360 (2)	2.45 (7)	2.19 (7)	2.69 (7)	−0.32 (6)	0.13 (6)	−0.28 (6)
N1	0.1183 (3)	−0.1045 (6)	0.3466 (5)	2.3 (2)	1.1 (2)	2.2 (2)	−0.0 (2)	0.3 (3)	−0.5 (2)
N2	−0.0081 (3)	0.0277 (7)	0.2272 (5)	1.6 (2)	2.3 (3)	2.1 (2)	−0.0 (2)	0.5 (3)	−0.3 (2)
N3	0.0535 (3)	0.1931 (7)	0.0572 (5)	2.2 (2)	2.0 (2)	2.2 (2)	−0.0 (2)	0.5 (2)	−0.3 (2)
C2	0.1871 (5)	−0.2872 (9)	0.4941 (7)	3.0 (3)	2.3 (3)	3.3 (3)	0.8 (3)	−0.9 (3)	−0.4 (3)
C1	0.1885 (4)	−0.1717 (9)	0.4002 (6)	2.0 (3)	3.2 (3)	2.8 (3)	0.7 (3)	−0.2 (2)	0.1 (3)
C3	0.1118 (5)	−0.3327 (9)	0.5339 (6)	3.5 (4)	2.7 (3)	2.6 (3)	0.6 (3)	−0.2 (3)	0.6 (3)
C4	0.0392 (4)	−0.2663 (9)	0.4818 (6)	3.1 (3)	2.4 (3)	2.4 (3)	0.1 (3)	0.9 (2)	−0.2 (3)
C5	0.0438 (4)	−0.1508 (8)	0.3874 (6)	1.5 (3)	2.5 (3)	2.4 (3)	−0.2 (2)	0.2 (2)	−0.2 (2)
C6	−0.0285 (4)	−0.0681 (8)	0.3221 (6)	1.9 (3)	1.6 (3)	2.6 (3)	−0.4 (2)	0.3 (2)	−0.6 (2)
C7	−0.1117 (4)	−0.0878 (8)	0.3492 (6)	2.4 (3)	2.2 (3)	3.0 (3)	−0.2 (3)	0.8 (2)	0.0 (3)
C8	−0.1714 (4)	−0.0012 (9)	0.2752 (7)	2.0 (3)	3.9 (3)	3.4 (4)	−0.3 (3)	0.5 (3)	−1.0 (3)
C9	−0.1503 (4)	0.0954 (9)	0.1769 (7)	2.1 (3)	3.2 (4)	2.9 (3)	0.3 (3)	−0.4 (2)	0.1 (3)
C10	−0.0663 (4)	0.1080 (8)	0.1568 (6)	2.1 (3)	1.5 (3)	2.4 (3)	0.1 (2)	0.1 (2)	−0.3 (2)
C11	−0.0303 (4)	0.2010 (8)	0.0559 (5)	2.7 (3)	2.2 (3)	2.0 (3)	−0.3 (2)	−0.0 (2)	−1.0 (2)
C12	−0.0784 (5)	0.2899 (9)	−0.0342 (6)	3.2 (4)	2.2 (3)	2.6 (3)	0.7 (3)	−0.1 (2)	−0.1 (2)
C13	−0.0372 (5)	0.3742 (9)	−0.1254 (7)	4.9 (4)	2.5 (3)	2.5 (3)	−0.0 (3)	−0.1 (2)	0.6 (3)
C14	0.0483 (5)	0.3679 (9)	−0.1225 (6)	4.6 (4)	2.1 (3)	2.3 (3)	−0.6 (3)	0.4 (3)	−0.5 (3)
C15	0.0922 (5)	0.2744 (9)	−0.0308 (7)	3.6 (4)	2.1 (3)	3.2 (3)	−0.7 (3)	1.3 (3)	−0.4 (3)

atom	x/a	y/b	z/c	B, Å²	atom	x/a	y/b	z/c	B, Å²
H1	0.243 (4)	−0.140 (8)	0.364 (6)	3 (2)	H9	−0.191 (3)	0.147 (7)	0.122 (5)	2 (1)
H2	0.236 (5)	−0.334 (11)	0.548 (8)	7 (2)	H12	−0.142 (4)	0.293 (9)	−0.038 (6)	4 (2)
H3	0.115 (4)	−0.430 (8)	0.592 (5)	2 (1)	H13	−0.065 (4)	0.426 (8)	−0.186 (5)	2 (1)
H4	−0.012 (4)	−0.296 (9)	0.499 (8)	5 (2)	H14	0.077 (4)	0.430 (9)	−0.179 (7)	4 (2)
H7	−0.121 (4)	−0.163 (8)	0.394 (6)	3 (2)	H15	0.145 (4)	0.264 (8)	−0.028 (5)	2 (1)
H8	−0.228 (4)	−0.005 (7)	0.293 (5)	2 (1)					

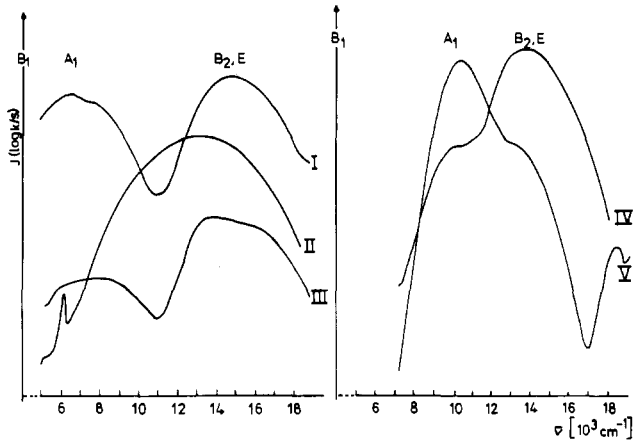

Figure 1. Reflection spectra of (I–III) $Cu(terpy)_mCl_2 \cdot nH_2O$ (298 K) (I, $m = 2$; II, $m = 1$ after drying over P_2O_5; III, after exposure to moist air), (IV) $Cu(terpy)Cl_2$ (4.2 K), and (V) $Cu(terpy)I_2$ (4.2 K). Band assignments for I, III, and IV are according to C_{4v} symmetry; sharp peaks below 6500 cm^{-1} are due to the terpyridine ligand.[1]

H, 2.3; N, 9.2. Calcd for X = I^-: C, 32.7; H, 2.0; N, 7.6. Found: C, 33.1; H, 1.9; N, 7.7.

X = NO_2^-. Green crystals of $Cu(terpy)(NO_2)_2 \cdot 2H_2O$ were obtained from aqueous solutions of $Cu(NO_2)_2$ and terpyridine. We prepared the copper salt by reacting $AgNO_2$ with $CuCl_2$. Anal. Calcd: C, 42.4; H, 3.6; N, 16.5. Found: C, 42.4; H, 3.2; N, 15.9.

X = NO_3^-. The reaction of $Cu(NO_3)_2 \cdot 3H_2O$ and terpyridine in water and subsequent recrystallization yielded blue needles, which become opaque without mother liquor. The analysis is in agreement with the constitution $Cu(terpy)(NO_3)_2 \cdot H_2O$. Anal. Calcd: C, 41.1; H, 3.0; N, 16.0. Found: C, 41.2; H, 2.8; N, 15.5. By drying the complex over P_2O_5 in vacuo, we obtained the anhydrous compound, which reversibly takes up water again in air.

X = F^-. CuF_2 dissolves readily in boiling water in the presence of terpyridine. Only by evaporating the dark green solution nearly to dryness did we obtain a very hygroscopic compound of the presumable constitution $Cu(terpy)F_2 \cdot nH_2O$.

Optical Measurements. The ligand field reflection spectra were recorded by a Zeiss PMQII spectrometer (Infrasil) with a low-temperature attachment. We used Sr_2ZnTeO_6 (4000–12 000 cm^{-1}) and freshly sintered MgO (8000–30 000 cm^{-1}) as standards.

EPR Measurements. The EPR spectra were taken with a Varian E15 spectrometer (35 and 9 GHz) at 298, 77, and 4.2 K. DPPH was used as internal standard ($g = 2.003_7$).

X-ray Structure Analysis of $Cu(terpy)Cl_2 \cdot nH_2O$ ($n = 0, 1$). A light green ($n = 0$) single crystal with the habit of a truncated pyramid and a dark green single crystal ($n = 1$) of column shape, both of about 0.01 mm^3 volume, were chosen for the structural analysis. The Laue symmetry was $2/m$ in both cases. The intensities were measured with an automated Philips PW 1100 four-cycle diffractometer at 298 K and the data collected up to $\theta \simeq 23°$ by a $\omega/2\theta$ scan technique (scan width 1.2°) using Mo Kα (0.710 69 Å) radiation (graphite monochromator). No absorption corrections were applied.

$n = 0$. From the experimental extinctions ($h0l$, $l = 2n$; $0k0$, $k = 2n$) the space group $P2_1/a$ could be uniquely deduced, which is easily transformable into $P2_1/c$ (No. 14). We obtained the cell dimensions by a least-squares fit of 14 reflections: $a = 16.088$ (8) pm, $b = 8.249$ (5) pm, $c = 10.680$ (4) pm, and $\beta = 94.66$ (3)° with $Z = 4$. The integral intensity and the background on both sides were measured for each reflection. From 4182 reflections 1669 remained that were symmetry independent. A total of 240 reflections had an intensity below the limit of observation: $F_{min} = 2\sigma(F)$ ($\sigma(F)$ is derived from the statistical standard deviation of a single measurement, $\sigma(I)$). They were included in the refinement but not in the calculation of the reliability factor $R = \sum||F_o| - |F_c||/\sum|F_o|$. The positional parameters of the heavy atom could be deduced from the Patterson map. The subsequent first isotropic refinement (X-ray system 72) led to $R = 0.34$. The difference Fourier syntheses yielded then all atoms in the asymmetric unit with the exception of the hydrogen atoms. Their positions were calculated with the assumption of a C–H bond length of 1 Å. The last isotropic refinement resulted in $R = 0.13$. The final anisotropic refinement (H atoms isotropic) led to $R = 0.054$. Of the 240 unobserved reflections only 2 were calculated to have intensities between $2\sigma(F)$ and $3\sigma(F)$. The final atomic and thermal parameters are given in Table I.

$n = 1$. The observed extinctions (hkl, $h + k = 2n + 1$; $h0l$, $l = 2n + 1$; $0k0$, $k = 2n + 1$) are compatible with the space groups $C2/c$ (No. 15) and Cc (No. 9). We decided to choose $C2/c$, because a test by means of Wilson statistics is in far better agreement with a centrosymmetrical space group. The analysis followed the same procedure as described for $n = 0$. While the H atoms of the terpyridine ligand were found in the Fourier map, the hydrogen atoms of the water molecule could not be detected. The dimensions of the monoclinic unit cell with $Z = 8$ are $a = 17.18$ (1) Å, $b = 9.54$ (1) Å, $c = 18.76$

Table II. Positional and Thermal Parameters for $Cu(terpy)Cl_2 \cdot H_2O$

atom	x/a	y/b	z/c	B_{11}	B_{22}	B_{33}	B_{12}	B_{13}	B_{23}
Cu1	0.30922 (2)	0.12094 (5)	0.07072 (2)	2.07 (2)	2.47 (2)	2.52 (2)	−0.36 (2)	0.43 (1)	0.09 (2)
Cl1	0.18399 (5)	0.0730 (1)	0.07824 (5)	1.92 (4)	3.74 (5)	3.70 (5)	−0.41 (3)	0.27 (3)	0.42 (4)
Cl2	0.37656 (5)	−0.0576 (1)	0.15883 (5)	2.88 (4)	3.80 (5)	3.26 (5)	0.73 (4)	0.41 (3)	0.93 (4)
N1	0.3232 (2)	0.2838 (3)	0.1415 (2)	2.5 (1)	2.5 (1)	2.6 (1)	−0.0 (1)	0.5 (1)	0.1 (1)
N2	0.4043 (2)	0.2055 (3)	0.0435 (1)	2.1 (1)	2.2 (1)	2.3 (1)	−0.1 (1)	0.3 (1)	0.3 (1)
N3	0.3217 (2)	0.0110 (3)	−0.0208 (2)	2.6 (1)	2.4 (1)	2.6 (1)	−0.3 (1)	0.2 (1)	0.2 (1)
C1	0.2760 (2)	0.3186 (4)	0.1905 (2)	3.4 (2)	3.1 (2)	3.1 (2)	0.1 (1)	0.8 (1)	0.4 (1)
C2	0.2939 (2)	0.4257 (4)	0.2394 (2)	4.2 (2)	3.7 (2)	3.2 (2)	0.8 (2)	0.9 (1)	−0.1 (2)
C3	0.3617 (2)	0.4992 (4)	0.2371 (2)	4.3 (2)	3.5 (2)	3.4 (2)	0.1 (2)	0.2 (2)	−0.8 (2)
C4	0.4106 (2)	0.4657 (4)	0.1861 (2)	3.3 (2)	3.1 (2)	3.6 (2)	−0.2 (1)	0.2 (1)	−0.3 (1)
C5	0.3901 (2)	0.3568 (4)	0.1395 (2)	2.5 (2)	2.5 (2)	2.4 (1)	0.0 (1)	−0.0 (1)	0.3 (1)
C6	0.4369 (2)	0.3109 (4)	0.0825 (2)	2.3 (1)	2.1 (1)	2.5 (2)	−0.1 (1)	0.1 (1)	0.2 (1)
C7	0.5063 (2)	0.3687 (4)	0.0663 (2)	2.5 (2)	2.7 (2)	3.7 (2)	−0.4 (1)	0.3 (1)	0.0 (1)
C8	0.5383 (2)	0.3175 (4)	0.0074 (2)	2.4 (2)	3.3 (2)	4.3 (2)	−0.3 (2)	0.7 (1)	0.5 (2)
C9	0.5026 (2)	0.2121 (4)	−0.0340 (2)	2.7 (2)	3.2 (2)	3.3 (2)	0.1 (1)	1.0 (1)	0.3 (1)
C10	0.4341 (2)	0.1565 (4)	−0.0143 (2)	2.5 (1)	2.4 (2)	2.5 (2)	0.3 (1)	0.4 (1)	0.4 (1)
C11	0.3861 (2)	0.0446 (4)	−0.0517 (2)	2.6 (1)	2.5 (2)	2.4 (2)	0.1 (1)	0.1 (1)	0.4 (1)
C12	0.4044 (2)	−0.0218 (4)	−0.1123 (2)	3.6 (2)	3.5 (2)	3.0 (2)	0.2 (2)	0.7 (1)	−0.2 (1)
C13	0.3556 (2)	−0.1272 (4)	−0.1420 (2)	5.0 (2)	3.9 (2)	3.2 (2)	0.1 (2)	0.3 (2)	−0.8 (2)
C14	0.2908 (2)	−0.1633 (4)	−0.1102 (2)	4.4 (2)	3.4 (2)	3.6 (2)	−0.7 (2)	−0.2 (2)	−0.5 (2)
C15	0.2756 (2)	−0.0910 (4)	−0.0497 (2)	3.3 (2)	3.2 (2)	3.3 (2)	−0.6 (1)	0.1 (1)	0.2 (1)
O1	0.50	0.1529 (5)	0.25	5.9 (2)	4.8 (2)	5.2 (2)	0	1.2 (2)	0
O2	0.0	0.2450 (5)	0.25	8.1 (3)	3.4 (2)	11.4 (4)	0	−5.5 (3)	0

atom	x/a	y/b	z/c	B, Å²	atom	x/a	y/b	z/c	B, Å²
H1	0.228 (2)	0.265 (4)	0.188 (2)	4 (1)	H9	0.526 (2)	0.179 (4)	−0.073 (2)	4 (1)
H2	0.257 (3)	0.450 (5)	0.274 (2)	6 (1)	H12	0.449 (2)	0.004 (4)	−0.133 (2)	5 (1)
H3	0.377 (2)	0.572 (4)	0.266 (2)	5 (1)	H13	0.369 (2)	−0.172 (5)	−0.183 (2)	6 (1)
H4	0.457 (2)	0.517 (4)	0.185 (2)	4 (1)	H14	0.256 (2)	−0.234 (5)	−0.126 (2)	6 (1)
H7	0.532 (2)	0.446 (4)	0.095 (2)	4 (1)	H15	0.234 (2)	−0.111 (4)	−0.025 (2)	4 (1)
H8	0.584 (3)	0.352 (5)	0.000 (3)	8 (1)					

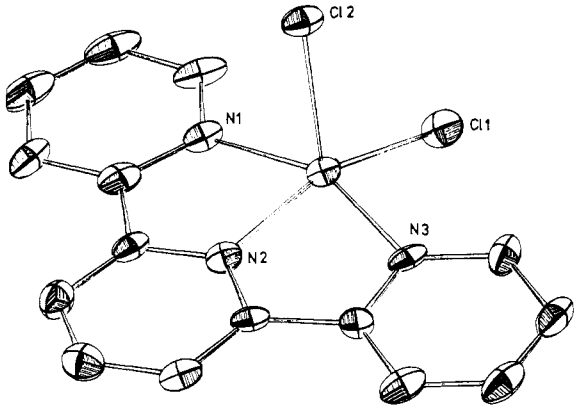

Figure 2. Geometry of $Cu(terpy)Cl_2$ polyhedra in $Cu(terpy)Cl_2 \cdot nH_2O$ (n = 0, 1).

(1) Å, and β = 96.8 (1)°. The total number of measured reflections is 4080 and the number of symmetry-independent reflections 2007. A total of 136 reflections had an intensity below $2\sigma(F)$. The final R value was 0.029. The atomic and thermal parameters are collected in Table II. The oxygen atom of the water molecule occupies two independent positions on the twofold axis.[21]

The scattering factors were taken from ref 7 for Cu, ref 8 for Cl and O, ref 9 for N and C_{val}, and ref 10 for H.

Results and Discussion

The Cu^{2+} ions are coordinated by the tridentate terpyridine molecule and the two Cl^- ions in both $Cu(terpy)Cl_2 \cdot nH_2O$ compounds (n = 0,1). The CuN_3Cl_2 geometries are best described as square pyramidal in reasonable approximation

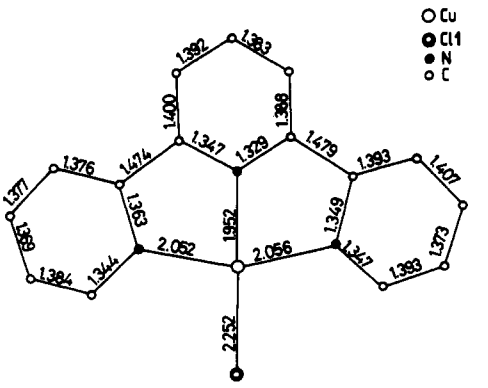

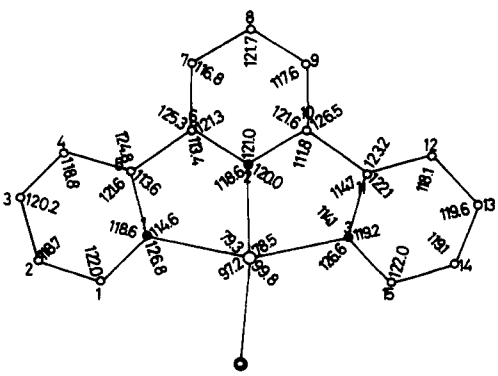

Figure 3. Bond lengths (above) and bond angles (below) for Cu(terpy)Cl_2: Cu–Cl2, 2.469 Å; ∠Cl2–Cu–Cl1, 104.5°; ∠Cl2–Cu–Ni ≡ α_i, α_1 = 99.5°, α_2 = 98.7°, α_3 = 92.4°. Standard deviations: σ(C–C) = 0.009 Å, σ(C–N) = 0.008 Å, σ(∠C–C(N)–C) = 0.9°, σ(Cu–N) = 0.005 Å, σ(Cu–Cl) = 0.002 Å, σ(∠N–Cu–N(Cl)) = 0.4°.

(Figure 2, Table III). The N atoms and one Cl^- ion represent the equatorial plane and are bonded in a relatively short

(7) D. T. Cromer and J. T. Waber, *Acta Crystallogr.*, **18**, 105 (1965).
(8) H. P. Hanson, F. Herman, J. D. Lea, and S. Skilman, *Acta Crystallogr.*, **17**, 1040 (1964).
(9) "International Tables for X-ray Crystallography", Vol. 3, Kynoch Press, Birmingham, England, 1972, Table 3.3 A.
(10) R. F. Stewart, E. R. Davidson, and W. T. Simpson, *J. Chem. Phys.*, **42**, 3175 (1965).

Table III. Local Symmetry of CuN_3Cl_2 Polyhedra in $Cu(terpy)Cl_2 \cdot nH_2O$[a]

	θ_{SP}[b]	θ_{TBP}[b]	Φ[b]	θ_0[c]	Φ_0[c]	θ_1[d]	Φ_1[d]	θ[e]	Φ[e]
N1	~100	90	90	99.$_5$	79	94.$_5$	80	97	78.$_5$
N2	~100	120	0	98.$_5$	0	96.$_5$	0	125	0
N3	~100	90	270	92.$_5$	280	96.$_5$	279.$_5$	97	281.$_5$
Cl1	~100	120	180	104.$_5$	181	101	179.$_5$	111	180
Cl2	0	0		0		0		0	

[a] θ, Φ = polar coordinates with respect to Cu–Cl2 bond direction (Figure 2). All coordinates are in degrees. [b] Values for ideal TBP and SP (Φ angles identical). [c] Values for $Cu(terpy)Cl_2 \cdot nH_2O$ with $n = 0$. [d] Values for $Cu(terpy)Cl_2 \cdot nH_2O$ with $n = 1$. [e] Values for $Co(terpy)(NCO)_2$[16] are included for comparison.

distance, while the apical Cl^- ligand is found in comparatively great distance from the central Cu^{2+} ion. Bond lengths and bond angles are given in Figures 3 and 4.[21] Because of the rigidity of the terpyridine ring the angles N2–Cu–N1 and N2–Cu–N3 deviate from 90° by about 10° and the Cu–N2 bond length is smaller than Cu–N1,3 by 0.1 Å. The average Cu–N distances (2.02 (2.01) Å for $n = 0$ (1)) are much smaller than the average Cu–N bond length in $Cu(terpy)_2(NO_3)_2$ (2.12 Å).[2] The same is true for the Cu–Cl1 bond (2.25 (2.22) Å for $n = 0$ (1)) in comparison to the average distances in $CuCl_5^{3-}$ polyhedra (2.35 Å).[3,11] On the other hand, the apical Cu–Cl2 bond is appreciably longer (2.47 (2.55) Å for $n = 0$ (1)). The evidence of a strongly "apically elongated" square-pyramidal coordination is supported by further structural results. $Cu(terpy)(CN)NO_3 \cdot H_2O$ crystallizes in the same space group as $Cu(terpy)Cl_2$ and contains also elongated SP's.[12] The CN^- ions bridge two polyhedra, in which the C atom is bonded in the equatorial plane (1.92 Å) and the N atom occupies the apical position in a quite large distance from Cu^{2+} (2.21 Å). The Cu–N1,2,3 bond lengths are the same as in the Cl^- compounds; the NO_3^- ion and the H_2O molecule are not bonded to Cu^{2+}. $Cu(terpy)(NO_2)_2 \cdot H_2O$ is especially interesting, because H_2O participates in the bonding to Cu^{2+}.[13] It is found in the long-distance apical position (2.24 Å), while one NO_2^- ion is bonded to Cu^{2+} in the equatorial plane via an O ligator atom (1.97 Å). The Cu–N bond lengths are again the same as in the Cl^- complexes (2.01 Å in the average). The second NO_2^- ion does not coordinate.

The comparison of the geometries of the CuN_3Cl_2 entities in $Cu(terpy)Cl_2 \cdot nH_2O$ with the corresponding Co^{2+} polyhedron in $Co(terpy)Cl_2$ (space group $P2_1/c$)[14] is quite informative. The Co^{2+} coordination is also approximately square pyramidal, but *no bond length anomalies* are observed. Though the ionic radii of high-spin Co^{2+} and Cu^{2+} are nearly identical, the average Co–N bond length (2.13 Å) is much larger than the comparable Cu–N distance. Also the two Co–Cl bond lengths are equal (2.29 Å) and rather intermediate between Cu–Cl1 and Cu–Cl2 in CuN_3Cl_2. Similar bond lengths as in $Co(terpy)Cl_2$ are found in $Zn(terpy)Cl_2$,[15] though the ZnN_3Cl_2 geometry is intermediate between SP and TBP. Finally the compound $Co(terpy)(NCO)_2$ demonstrates that the tridentate ligand can also accommodate a trigonal-bipyramidal coordination with the N atoms in one equatorial and the two axial positions. The difference in geometry between the CoN_5 polyhedron in the mentioned compound and the CuN_3Cl_2 entities is clearly demonstrated, if polar coordinates are used (Table III). Again bond length anomalies (2.11$_5$ Å (ter-

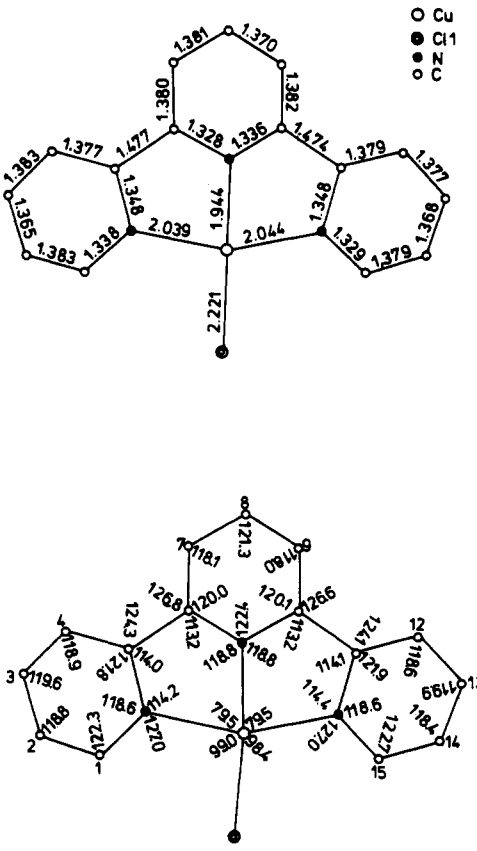

Figure 4. Bond lengths (above) and bond angles (below) for Cu(terpy)$Cl_2 \cdot H_2O$: Cu–Cl2, 2.554 Å; ∠Cl2–Cu–Cl1, 100.9°; ∠Cl2–Cu–Ni ≡ α_i, α_1 = 94.4°, $\alpha_2 = \alpha_3$ = 96.7°. Standard deviations: σ(C–C) = 0.005 Å, σ(C–N) = 0.004 Å, σ(∠C–C(N)–C) = 0.3°, σ(Cu–N) = 0.003 Å, σ(Cu–Cl) = 0.001 Å, σ(∠N–Cu–N(Cl)) = 0.1°.

pyridine, 3×) and 1.95 Å (NCO^-, 2×))[16] are not observed in the CoN_5 polyhedron. We may conclude that in the compounds $Cu(terpy)X_2 \cdot nH_2O$ with five-coordinated Cu^{2+} polyhedra the apically elongated SP is the energetically preferred geometry.

While each of the three pyridine rings in the compounds $Cu(terpy)Cl_2 \cdot nH_2O$ is planar, they are slightly inclined toward each other by 6° at the most within the terpyridine frame. The N1 and N3 atoms deviate from the best equatorial plane by nearly 0.1 Å ($n = 0$) and 0.05 Å ($n = 1$) and the N2 and Cl1 atoms by about –0.1 Å ($n = 0$) and –0.05 Å ($n = 1$). The Cu^{2+} ions lie 0.26 Å ($n = 0$) and 0.33 Å ($n = 1$) above this plane. Obviously the CuN_3Cl_2 polyhedron in $Cu(terpy)Cl_2 \cdot H_2O$ deviates less from a regular square pyramid than the one in the anhydrous compound (compare also the polar coordinates in Table III). This argument is probably the reason for the comparatively larger difference between apical and equatorial Cu–Cl bond lengths in $Cu(terpy)Cl_2 \cdot H_2O$. It is not easy to find an explanation for these slightly different local geometries, however. Possibly hydrogen bonding between Cl2 and H_2O induces an elongation of the apical Cu–Cl2 bond length. Though we were not able to localize the hydrogen positions of the water molecule in the Fourier maps, the O–Cl2 distances of 3.2 Å are short enough indeed to give a strong argument.

The positions of the four CuN_3Cl_2 square pyramids in the unit cell of the anhydrous compound—projected into the *bc* plane—are shown in Figure 5. The polyhedra around Cu1 and Cu2 as well as Cu3 and Cu4 are connected by an inversion center with an antiparallel orientation of the long Cu–Cl2 axes. The angle between the Cu1–Cl2 and Cu3,4–Cl2 bond direc-

(11) K. N. Raymond, D. W. Meek, and J. A. Ibers, *Inorg. Chem.*, **7**, 1111 (1968).
(12) O. P. Anderson, A. B. Packard, and M. Wicholas, *Inorg. Chem.*, **15**, 1613 (1976).
(13) R. Allmann, S. Kremer, and D. Kucharczyk, to be submitted for publication.
(14) E. Goldschmied and N. C. Stephenson, *Acta Crystallogr., Sect. B*, **B26**, 1867 (1970).
(15) F. W. B. Einstein and B. R. Penfold, *Acta Crystallogr.*, **20**, 924 (1966).
(16) D. L. Kepert, E. S. Kucharski, and A. H. White, *Inorg. Chem.*, **19**, 1932 (1980).

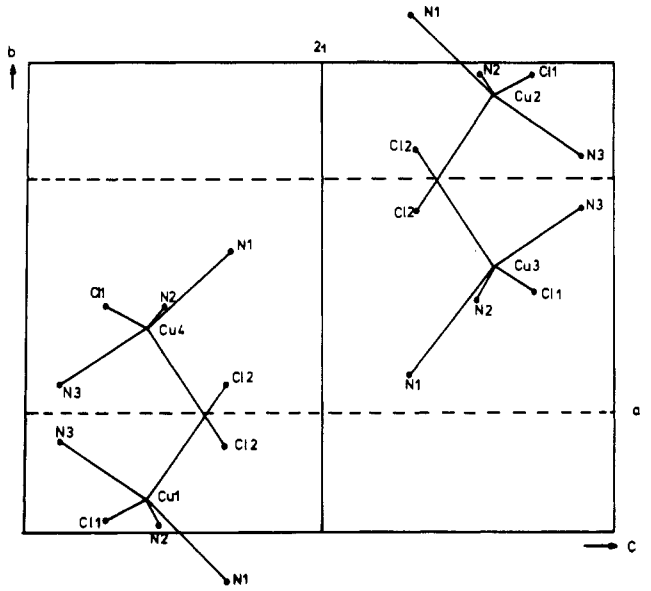

Figure 5. Projection of the four CuN_3Cl_2 polyhedra in the unit cell of $Cu(terpy)Cl_2$ into the (100) plane.

tions (Cu1–Cu3 distance 7.54, Cu1–Cu4 distance 8.59 Å) is $2\epsilon' = 68.4°$, however. Though two signals are thus expected in a single-crystal EPR experiment, only one **g** tensor is observed. Hence, it seems reasonable to assume that the two sublattices Cu1 and Cu3 (Cu2 and Cu4) with a distance below 8 Å are exchange coupled.[17] The experimental g values are $g_1^{ex} = 2.18_8$, $g_2^{ex} = 2.13_5$, and $g_3^{ex} = 2.07_0$ (298 and 77 K; $\bar{g} = 2.13_1$) (Figure 6). They obviously do not reflect the approximate square-pyramidal geometry of the CuN_3Cl_2 entity, because the following molecular g values are expected for a $d_{x^2-y^2}$ ground state in C_{4v} symmetry:

$$g_\parallel = g_z = g_0 + 8u_\parallel \qquad g_\perp = g_x = g_y = g_0 + 2u_\perp \tag{1}$$

Exchange interactions between differently oriented polyhedra with the canting angle 2ϵ[18] will induce a coupled **g** tensor, however:

$$\begin{aligned} g_1^{ex} &= (\cos^2\epsilon)g_\parallel + (\sin^2\epsilon)g_\perp \\ g_2^{ex} &= (\sin^2\epsilon)g_\parallel + (\cos^2\epsilon)g_\perp \qquad g_3^{ex} = g_\perp \end{aligned} \tag{2}$$

For $2\epsilon = 90°$ ("antiferrodistortive order"[19] of SP's) eq 2 simplifies to

$$g_\parallel^{ex} = g_\perp \qquad g_\perp^{ex} = \tfrac{1}{2}(g_\parallel + g_\perp) \tag{2a}$$

The canting angle 2ϵ is easily calculated from the exchange-narrowed **g** tensor of eq 2:

$$\cos 2\epsilon = \frac{g_1^{ex} - g_2^{ex}}{g_1^{ex} + g_2^{ex} - 2g_3^{ex}} \tag{2b}$$

We obtain $2\epsilon = 73°$, in reasonable agreement with the crystallographic value of $2\epsilon'$.[18] The resulting molecular **g** tensor is $g_\parallel = 2.25_3$, $g_\perp = 2.07_0$. The sequence $g_\parallel > g_\perp > g_0$ indeed

(17) A direct Cu^{2+}–Cu^{2+} exchange is rather improbable. The exchange presumably occurs via an overlap between the spacious terpyridine rings of different $Cu(terpy)L_2$ polyhedra. The Cu–Cu distances may be useful as rough orientations concerning the strength of the electronic interaction but give no information concerning the superexchange pathway.

(18) Because the $g_\perp$ components of an axial molecular **g** tensor are presumably located in the best equatorial plane, 2ϵ is defined as the canting angle between the normals to the equatorial planes of two interacting polyhedra, which is not necessarily equal to $2\epsilon'$ ($2\epsilon'$ = crystallographic canting angle between the long axes of two interacting square pyramids).

(19) D. Reinen and C. Friebel, *Struct. Bonding (Berlin)*, **37**, 1 (1979).

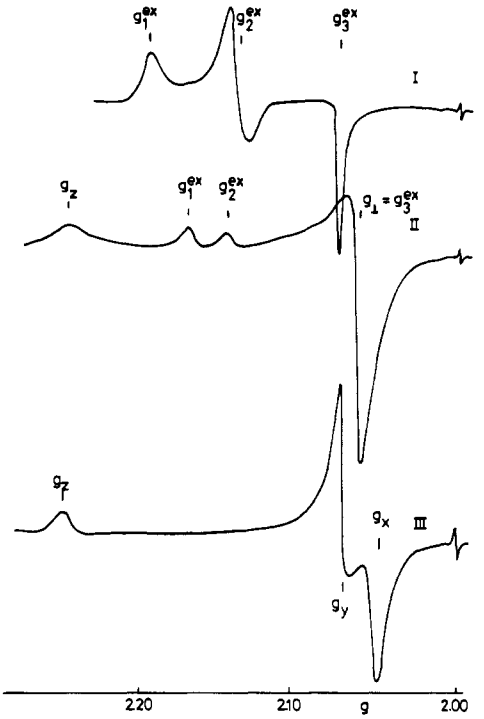

Figure 6. EPR powder spectra of $Cu(terpy)Cl_2 \cdot nH_2O$ (I, $n = 0$; II, $n = 1$) and $Cu(terpy)(NO_2)_2 \cdot 2H_2O$ (III).

reflects eq 1 and is indicative of a $d_{x^2-y^2}$ ground state. A trigonal-bipyramidal geometry demands $g_\perp > g_\parallel \simeq g_0$. The **g** tensor in this case is explicitly

$$g_\parallel = g_0 \qquad g_\perp = g_0 + 6u_\perp \tag{3}$$

Though the symmetry of the CuN_3Cl_2 polyhedra deviates significantly from C_{4v}, we have based our calculation on the assumption of regular square pyramids. Presumably the molecular **g** tensor is slightly orthorhombic, however (see below). The 298 K ligand field spectrum shows a broad band at $\simeq 13\,000$ cm^{-1}, which resolves into a peak at 13 200 cm^{-1} and a distinct shoulder at 10 200 cm^{-1} at 5 K (Figure 1). We tentatively assign these bands to the nonresolved transitions $B_1 \rightarrow B_2$, E ($\Delta_\parallel$, $\Delta_\perp$) and to $B_1 \rightarrow A_1$ in C_{4v} symmetry, respectively. With these energies we can estimate the covalency factors from the orbital contributions u_i (eq 1)

$$u_i = \frac{k_i^2\lambda_0}{\Delta_i} \quad (i = \parallel, \perp;\ \lambda_0 = 830\ cm^{-1}) \tag{1a}$$

and obtain $k \approx 0.72$.

$Cu(terpy)Cl_2 \cdot H_2O$ contains eight CuN_3Cl_2 polyhedra in the unit cell. Between four of them the same symmetry relations as described for the anhydrous compounds are valid, but with a canting angle $2\epsilon' = 83.7°$. The four additional Cu^{2+} polyhedra are generated by the translation ($^1/_2$, $^1/_2$, 0) and do not represent new orientations. The shortest distance between polyhedra connected by $2\epsilon'$ is 8.7 Å. The single-crystal EPR experiment yields two signals in all directions as expected for two nonequivalent orientations of the eight polyhedra. The powder g values are $g_\perp = 2.23_8$, $g_\perp = 2.06_2$ (298, 77, and 4.2 K; $\bar{g} = 2.12_1$). The two additional weak signals with g values of 2.13_8 and 2.16_1, which are only visible in the powder spectrum (Figure 6), can be understood as being induced by exchange interaction between the two EPR spectroscopically nonequivalent sites with a distance of 8.7 Å ($g_1^{ex} = 2.16_1$, $g_2^{ex} = 2.13_8$, $g_3^{ex} = 2.06_2$; $\bar{g} = 2.12_0$) and are indeed well reproduced by applying eq 2 with the crystallographic $2\epsilon'$ angle. At present we have no explanation for the simultaneous presence of molecular and cooperative g values, however. $g_\perp$ is split into two components ($\delta g \simeq 0.01$) in the single-crystal

measurement. The ligand field absorption—a strong band at 14 500 cm^{-1} and a shoulder at about 11 000 cm^{-1} (5 K)—is distinctly shifted to higher energies compared to the signal for the anhydrous compound, in agreement with the smaller average g value and the larger difference between the apical and equatorial bond length in the case of $Cu(terpy)Cl_2 \cdot H_2O$. The covalency parameter is again $k \approx 0.72$. Though a hyperfine structure is not resolved in the single-crystal and powder spectra of $Cu(terpy)Cl_2 \cdot nH_2O$, line-width considerations support the given arguments. ΔH_{pp} varies from 120 G ($g_\parallel$) to 6 G ($g_\perp$) for the complex with $n = 1$, while the line width in the case of the anhydrous compound is only 10 G for g_3^{ex} and about 40 G for g_1^{ex}, g_2^{ex}. The presence of exchange interactions ($n = 0$) should indeed lead to an apparent narrowing of the EPR signal,[20] which is maximum in the direction of the lowest g value, g_3^{ex} (connected with $A_\perp$; $A_\perp < A_\parallel$). In the case of uncoupled polyhedra the unresolved hyperfine splitting is expected to induce compartively broader signals, in particular in the $g_\parallel$ direction (connected with $A_\parallel$). The observed line widths are in accord with these arguments and confirm the presence of exchange narrowing in the EPR spectra of the anhydrous complex.

Single crystals of $Cu(terpy)Br_2$ with a presumable CuN_3Br_2 coordination exhibit only one EPR signal. The powder spectrum is orthorhombic with g values of 2.24_0, 2.12_5, and 2.03_2 ($\bar{g} = 2.13_2$). Because the line-width effects are very similar to those of $Cu(terpy)Cl_2 \cdot H_2O$, the **g** tensor is presumably molecular. The large anisotropy of the two lower g values would indicate a geometry rather intermediate between a square pyramid and a trigonal bipyramid for the CuN_3Br_2 polyhedron. A final decision, whether the EPR spectrum reflects the molecular geometry or is exchange narrowed, is not possible, however, because crystallographic data are lacking. The ligand field spectrum shows a broad asymmetric transition at $\simeq$12 000 cm^{-1}. The **g** tensor of $Cu(terpy)I_2$ is also orthorhombic: 2.20_6, 2.11_0, 2.06_6 ($\bar{g} = 2.12_6$). The single-crystal spectra show only one signal with line-width magnitudes and variations comparable to those of $Cu(terpy)Cl_2$. Hence, the assumption of exchange narrowing seems reasonable, though the structure is not known yet. The broad ligand field band at 298 K is resolved at 5 K into a quite narrow transition at 10 200 cm^{-1} and a shoulder on the high-energy side at 12 700 cm^{-1} (Figure 1). The reverse intensity ratios of the two bands compared to the spectrum of $Cu(terpy)Cl_2$ are striking and possibly indicate significant deviations from the SP geometry. The unit cell of $Cu(terpy)(NO_2)_2 \cdot 2H_2O$ (space group $P\bar{1}$)[13] contains two $CuN_3(OH_2)(ONO)$ polyhedra, which are connected by an inversion center. Accordingly, only one signal occurs in the single-crystal EPR spectra, which show line-width effects similar to those for $Cu(terpy)Cl_2 \cdot H_2O$. Hence, the observed **g** values reflect the local geometry ($g_z = 2.24_3$, $g_y = 2.06_6$, $g_x = 2.04_7$ (298, 4.2K); $\bar{g} = 2.11_9$ (Figure 6)). The orthorhombic component is due to the deviation from C_{4v} symmetry. The **g** tensor is very similar to the one observed for $Cu(terpy)Cl_2 \cdot H_2O$, though an orthorhombic component is resolved in this case. With the energy of the broad ligand field band ($\simeq$15 700 cm^{-1}), a covalency parameter $k \simeq 0.74_5$ is estimated (eq 1, 1a). As expected for the substitution of two Cl by two O ligands, a value slightly higher than that calculated for the CuN_3Cl_2 polyhedra results. The **g** tensor of $Cu(terpy)(NO_3)_2 \cdot H_2O$ resembles that of the nitrito complex ($g_z = 2.25$ (broad signal), $g_y = 2.06_0$, $g_x = 2.05_3$; $\bar{g} = 2.12$). The main absorption band is centered around 14 800 cm^{-1}, with a shoulder around 12 000 cm^{-1} (5 K). One may suggest that H_2O coordinates in the basal plane of a CuN_3O_2 square pyramid, in which the apical position is occupied by a weakly bonded NO_3^- ion. The IR spectrum is not in contradiction with this assumption. It is further interesting to note that the abstraction of water by P_2O_5 changes the EPR spectrum appreciably. An obviously exchange-narrowed **g** tensor with the components 2.18_5, 2.13_3, and 2.07_1 ($\bar{g} = 2.13_0$) is observed.

We have finally collected spectroscopic data for $[Cu(terpy)CN]NO_3 \cdot H_2O$. The space group ($P2_1/c$)[12] is equivalent to that of $Cu(terpy)Cl_2$. The Cu1–Cu3,4 distances (compare Figure 5) are 5.21 and 8.90 Å, respectively. As in $Cu(terpy)Cl_2$ only one narrow signal is observed in the single-crystal EPR experiment. Obviously the **g** tensor (2.15_8, 2.10_6, 2.05_5) is cooperative, induced by an exchange coupling between Cu1 and Cu3—in analogy to $Cu(terpy)Cl_2$. From the experimental g values ($\bar{g} = 2.10_6$) the canting angle $2\epsilon = 70.3°$ is calculated (eq 2), which is in good agreement with the crystallographic value $2\epsilon' = 72.2°$ between the long apical Cu–N axes of the two EPR spectroscopically nonidentical Cu1 and Cu3 polyhedra in the unit cell.[18] The molecular g values, calculated from eq 2b, are $g_\parallel = 2.20_9$ and $g_\perp = 2.05_5$. Corresponding to the small average g value and the strong equatorial (CuN_3C) and weak apical Cu–ligand bonding, the ligand field band is found at 16 000 cm^{-1}, with a weak shoulder at about 12 000 cm^{-1}. The covalency parameter is $k \simeq 0.71$.

As we will demonstrate in the second paper of this series,[3] the square pyramid with short equatorial bond lengths and a strongly elongated apical bond length is the energetically slightly preferred geometry of CuL_5 polyhedra with respect to a compressed trigonal bipyramid. This statement is supported by the experimental findings for the class of compounds $Cu(terpy)X_2 \cdot nH_2O$, presented above. The terpyridine ligand is very rigid, however, and induces significant deviations from C_{4v} symmetry. Explicitly, the bond angle N1–Cu–N3 is always 155 ± 5° in the octahedral and the five-coordinate complexes discussed above. Also the T^{II}–N2 bond length is usually significantly shorter than the T^{II}–N1,3 spacings. Principally, the terpyridine frame can accommodate not only a square pyramid (coordination in the equatorial plane (Figure 2)) but also a trigonal bipyramid (coordination in the axial and one equatorial position), as was found in $Co(terpy)(NCO)_2$[16] for example. Deviations from the square-pyramidal geometry may eventually occur, if weak X ligands are coordinated. Possible examples are the $CuN_3(Br,I)_2$ polyhedra discussed before for which unfortunately crystallographic data are not available at present. A structural analysis at 298 K may sometimes be misleading, because a coordination geometry is presented that is only the dynamic average of polyhedra with quite different symmetries. In these cases EPR spectroscopy is the method of choice, which can unambigously discriminate between the different dynamic or static coordination alternatives via the electronic ground states. Sometimes the **g** tensor is severely influenced by exchange interactions, however, which give rise to complications. We have demonstrated by comparison with structural data that it is even then often possible to evaluate the molecular **g** tensors.

Registry No. I, 51063-22-0; II, 84894-25-7; III, 86471-86-5; $Cu(terpy)Br_2$, 25971-38-4; $Cu(terpy)I_2$, 25970-66-5; $Cu(terpy)(NO_3)_2 \cdot H_2O$, 86471-88-7; $Cu(terpy)F_2$, 86471-89-8.

(20) A. Abragam and B. Bleaney, "Electron Paramagnetic Resonance of Transition Ions", Clarendon Press, Oxford, England, 1970, p 508.

(21) Parallel to our work, a structure determination on $Cu(terpy)Cl_2 \cdot H_2O$ was published with analogous results, though the bond lengths and angles differ slightly, due to a higher R value (0.065): T. Rojo, M. Vlasse, and D. Beltranporter, *Acta Crystallogr., Sect. C*, **C39**, 194 (1983).